HAL open science

Modelling crack growth by level sets in the extended finite element method

Mariola Kurowska-Stolarska, David Chopp, Nicolas Moës, Ted Belytschko

To cite this version:

Mariola Kurowska-Stolarska, David Chopp, Nicolas Moës, Ted Belytschko. Modelling crack growth by level sets in the extended finite element method. International Journal for Numerical Methods in Engineering, 2001, 51 (8), pp.943-960. 10.1002/nme.201 . hal-01007079

HAL Id: hal-01007079

https://hal.science/hal-01007079v1

Submitted on 11 Jan 2023

HAL is a multi-disciplinary open access archive for the deposit and dissemination of scientific research documents, whether they are published or not. The documents may come from teaching and research institutions in France or abroad, or from public or private research centers.

L'archive ouverte pluridisciplinaire **HAL**, est destinée au dépôt et à la diffusion de documents scientifiques de niveau recherche, publiés ou non, émanant des établissements d'enseignement et de recherche français ou étrangers, des laboratoires publics ou privés.

Distributed under a Creative Commons Attribution - NonCommercial 4.0 International License

Modelling crack growth by level sets in the extended finite element method

M. Stolarska[1,*,†], D. L. Chopp[1], N. Moës[2] and T. Belytschko[2]

[1] *Department of Engineering Sciences and Applied Mathematics, Northwestern University, Evanston, IL 60208, U.S.A.*
[2] *Department of Mechanical Engineering, Northwestern University, Evanston, IL 60208, U.S.A.*

An algorithm which couples the level set method (LSM) with the extended finite element method (X-FEM) to model crack growth is described. The level set method is used to represent the crack location, including the location of crack tips. The extended finite element method is used to compute the stress and displacement fields necessary for determining the rate of crack growth. This combined method requires no remeshing as the crack progresses, making the algorithm very efficient. The combination of these methods has a tremendous potential for a wide range of applications. Numerical examples are presented to demonstrate the accuracy of the combi ned methods.

KEY WORDS: extended finite elements method; level set method; crack growth

1. INTRODUCTION

In this paper, we describe an algorithm where the level set method (LSM) is coupled with the extended finite element method (X-FEM) [1–3] to model crack growth. The LSM is a numerical scheme developed by Osher and Sethian [4] to model the motion of interfaces. In the LSM the interface is represented as the zero level set of a function of one higher dimension. The current formulation of the LSM has no provision for modelling free moving endpoints on curves or free moving edges on surfaces. A similar level set representation was used in Reference [5] to model the evolution of a curve segment. However, unlike the method presented here, in Reference [5] the endpoints of the evolving curve segment remain fixed. We present an extension of the LSM for modelling the evolution of an open curve segment and use this extension to model the growth of a fatigue crack.

*Correspondence to: Magdalena Stolarska, Department of Engineering Sciences and Applied Mathematics, Northwestern University, 2145 Sheridan Road, Evanston, IL 60208, U.S.A.
†E-mail: asm577@northwestern.edu

Contract/grant sponsor: Office of Naval Research

The X-FEM algorithm enables the modelling of crack growth without remeshing. In order to incorporate stress and displacement fields which are discontinuous across the crack, the mesh in previous formulations of the finite element method had to be adapted so that the crack coincided with the element edges. In contrast, the X-FEM algorithm allows for the crack to pass arbitrarily through elements by incorporating enrichment functions to handle the field discontinuities. In this manner the mesh can remain fixed throughout the evolution of the crack.

Alternative methods which address the issue of discontinuous elements have been proposed in References [6–9]. X-FEM differs from the first two in that there are no incompatibilities in the displacements between elements. In Reference [9], the visibility criterion developed in EFG [10] is used.

The LSM and X-FEM work well, offering complimentary capabilities. The level set representation of the crack simplifies the selection of the enriched nodes, as well as the definition of the enrichment functions. In addition to modelling the crack growth problem, the combined methods were also used to model holes and material inclusions in Reference [11] and three-dimensional planar crack growth in Reference [12]. The LSM and X-FEM, as described in this paper, provide a simple and efficient algorithm for modelling two-dimensional crack growth. Moreover, the coupling of the LSM with X-FEM will provide a simple and natural method for extending the crack growth model into three dimensions.

In Section 2, we discuss the model for crack propagation. In Sections 3 and 4, respectively, we give general descriptions of the LSM and X-FEM. In Section 5, the algorithm for modelling crack growth using a level set formulation is presented. In Section 6, we discuss the coupling of the LSM and X-FEM. In Section 7, we present some numerical results, and in Section 8, we conclude with a discussion.

2. GOVERNING EQUATIONS

In this section we will review the governing equations for the displacement field in an elastostatic analysis. The domain of the problem is Ω with boundary Γ. The boundary Γ is subdivided into two parts, Γ_u and Γ_t. The displacement is prescribed on Γ_u, and the traction is prescribed on Γ_t. In addition to the external boundary, the crack surface presents an additional boundary inside Ω. The crack surface is denoted by Γ_c and is traction free; Γ_c consists of Γ_c^+ and Γ_c^-, two coincident surfaces. The domain Ω and its boundary Γ are illustrated in Figure 1.

The strong form of the equilibrium equations and boundary conditions is

$$\nabla \cdot \boldsymbol{\sigma} + \mathbf{b} = 0 \quad \text{in } \Omega \tag{1}$$

$$\boldsymbol{\sigma} \cdot \mathbf{n} = \mathbf{T} \quad \text{on } \Gamma_t \tag{2}$$

$$\boldsymbol{\sigma} \cdot \mathbf{n} = 0 \quad \text{on } \Gamma_{c+} \tag{3}$$

$$\boldsymbol{\sigma} \cdot \mathbf{n} = 0 \quad \text{on } \Gamma_{c-} \tag{4}$$

$$\mathbf{u} = \mathbf{U} \quad \text{on } \Gamma_u \tag{5}$$

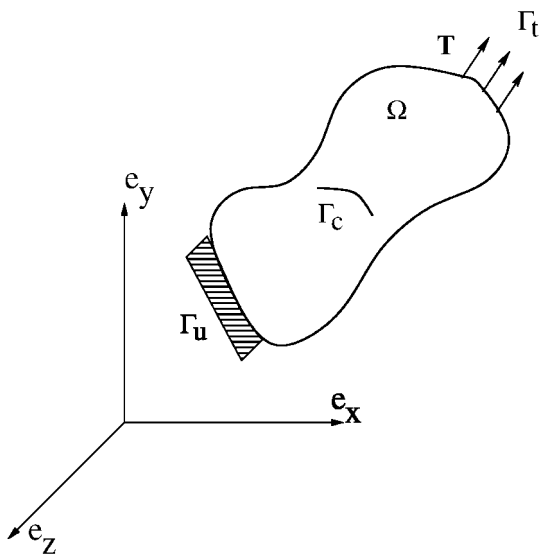

Figure 1. Domain Ω and its boundaries Γ.

where $\boldsymbol{\sigma}$ is the Cauchy stress tensor, $\mathbf{u}$ is the displacement, $\mathbf{b}$ is the body force per unit volume, and $\mathbf{n}$ is the unit outward normal. The prescribed traction and displacement are, respectively, $\mathbf{T}$ and $\mathbf{U}$.

We consider small strains and displacements, so the strain-displacement relation is

$$\boldsymbol{\varepsilon} = \boldsymbol{\varepsilon}(\mathbf{u}) = \boldsymbol{\nabla}_s \mathbf{u} \tag{6}$$

In Equation (6), $\boldsymbol{\nabla}_s$ is the symmetric part of the gradient, and $\boldsymbol{\varepsilon}$ is the linear strain tensor. The constitutive relation is given by Hooke's Law,

$$\boldsymbol{\sigma} = \mathbf{C} : \boldsymbol{\varepsilon} \tag{7}$$

where $\mathbf{C}$ is the Hooke tensor.

The space of admissible displacement fields is given by

$$\mathscr{U} = \{\mathbf{u} = \mathbf{U} \text{ on } \Gamma_u,\ \mathbf{u} \text{ is } C^0 \text{ and discontinuous on } \Gamma_c\} \tag{8}$$

The test space is given by

$$\mathscr{U}_0 = \{\mathbf{v} = 0 \text{ on } \Gamma_u,\ \mathbf{v} \text{ is } C^0 \text{ and discontinuous on } \Gamma_c\} \tag{9}$$

The weak form of the equilibrium equation is

$$\int_\Omega \boldsymbol{\varepsilon}(\mathbf{u}) : \mathbf{C} : \boldsymbol{\varepsilon}(\mathbf{v})\, d\Omega = \int_\Omega \mathbf{b} \cdot \mathbf{v}\, d\Omega + \int_{\Gamma_t} \mathbf{T} \cdot \mathbf{v}\, d\Gamma \quad \forall \mathbf{v} \in \mathscr{U}_0 \tag{10}$$

It is shown in Reference [2] that for these test and trial functions, the weak form, (10), implies the traction-free conditions on the crack surface Γ_c, (3) and (4), and the rest of the strong form as described in Equations (1)–(5).

3. THE LEVEL SET METHOD (LSM)

The LSM is a numerical technique for tracking the motion of interfaces. In this method, the interface of interest is represented as the zero level set of a function $\phi(\mathbf{x}(t),t)$. This function is one dimension higher than the dimension of the interface. The evolution equation for the interface can then be expressed as an equation for the evolution of ϕ. For our purposes, cracks will be considered as one-dimensional manifolds in two-dimensional space.

In general, a moving interface $\gamma(t)\subset\mathbb{R}^2$ can be formulated as the level set curve of a function $\phi(\mathbf{x},t):\mathbb{R}^2\times\mathbb{R}\rightarrow\mathbb{R}$, where

$$\gamma(t)=\{\mathbf{x}\in\mathbb{R}^2:\phi(\mathbf{x},t)=0\} \tag{11}$$

The motion of $\gamma(t)$ is translated into an evolution equation for ϕ by taking the time derivative of $\phi(\mathbf{x}(t),t)=0$. The resulting equation for the evolution of ϕ, and therefore γ, is

$$\phi_t+F\|\nabla\phi\|=0 \tag{12}$$

$$\phi(\mathbf{x},t=0)=\text{given} \tag{13}$$

where F is the speed of the front at $\mathbf{x}\in\gamma(t)$ in the direction normal to the interface. The initial conditions on ϕ are typically defined as

$$\phi(\mathbf{x},t)=\pm\min_{x_\gamma\in\gamma(t)}\|\mathbf{x}-\mathbf{x}_\gamma\| \tag{14}$$

where ϕ is the signed-distance to the interface. The sign of the minimum distance depends on which side of the interface a point $\mathbf{x}$ is located.

There are many advantages to using the LSM for tracking interfaces. First, unlike many other interface tracking schemes, the motion of the interface is computed on a fixed mesh. Second, the method handles changes in the topology of the interface naturally. Third, the evolution equation is of the form (12) regardless of the dimension of the interface. Hence, extending the method to higher dimensions is easily accomplished. Finally, the geometric properties of the interface can be obtained from the level set function ϕ. For example, the unit normal to the interface is given by $\mathbf{n}=\nabla\phi/\|\nabla\phi\|$.

One drawback to the LSM is that the level set representation requires a function of a higher dimension than the original crack, potentially leading to higher storage and computational costs. However, as noted in Reference [13], since we are only interested in motion near the interface, level set computation need only be done in a region surrounding it. This is done by first locating the interface and building the level set function using (14) in a predetermined region on either side of the interface. The level set function is then updated only in this region called the narrow band.

In two dimensions, the LSM has typically been used to track interfaces which are either closed curves or curves that extend to the boundary of the computational domain. To represent interfaces which are open segments, the level set model needs to be extended. A crack is represented as the zero level set of a function $\psi(\mathbf{x},t)$. The endpoints of the crack will be represented by the intersection of the zero level sets of two functions, $\psi(\mathbf{x},t)$ and $\phi_i(\mathbf{x},t)$, where the subscript i corresponds to the ith endpoint. The general formulation for tracking

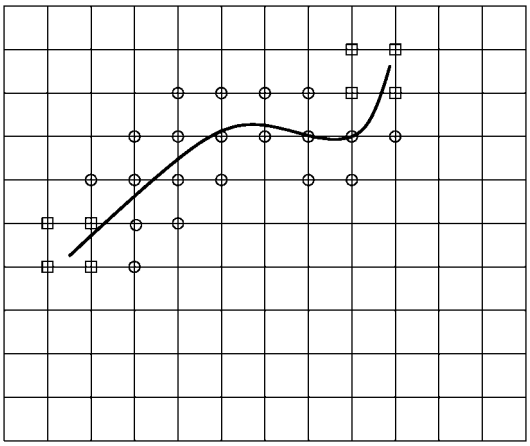

Figure 2. The set of nodes elected for enrichment. The nodes enriched by the branch function B_l are in squares. The nodes enriched by the Heaviside function H are circled.

open curves using level sets and its application to the representation of a crack is described in more detail in Section 5.

4. THE EXTENDED FINITE ELEMENT METHOD

Modelling crack growth in a traditional finite element framework is cumbersome due to the need for the mesh to match the geometry of the discontinuity. Many methods require remeshing of the domain at each time step. In X-FEM the need for remeshing is eliminated. The mesh does not change as the crack grows and is completely independent of the location and geometry of the crack. The discontinuities across the crack are modelled by enrichment functions.

To illustrate this, consider the X-FEM displacement approximation for a vector valued function $\mathbf{u}(\mathbf{x}) : \mathbb{R}^2 \to \mathbb{R}^2$ given by

$$\mathbf{u}^h(\mathbf{x},t) = \sum_{i\in I} \mathbf{u}_i(t)N_i(\mathbf{x}) + \sum_{j\in J} \mathbf{b}_j(t)N_j(\mathbf{x})H(\psi(\mathbf{x},t)) + \sum_{k\in K} N_k(\mathbf{x}) \left(\sum_{l=1}^{4} \mathbf{a}_k^l(t)B_l(r,\theta) \right) \tag{15}$$

where $N_i(\mathbf{x})$ is the shape function associated with node i and t is the time. Time in this class of problems is any monotonically increasing parameter; all solutions are for the equilibrium equations since dynamic effects are not considered. In Equation (15), J is the set of all nodes whose support is bisected by the crack. In Figure 2, this set is indicated by the circled nodes. The set K contains all the nodes of the elements containing the crack tip. This set is shown in Figure 2 by the nodes in squares. The nodal degrees of freedom corresponding to the displacement are $\mathbf{u}_i$, $\mathbf{b}_j$, and $\mathbf{a}_k$.

The second important and distinguishing factor to note in Equation (15) is the enrichment functions $H(\psi(\mathbf{x},t))$ and $B_l(r,\theta)$. The function $H(y)$ is defined as

$$H(y)=\begin{cases} 1 & \text{for } y>0 \\ -1 & \text{for } y<0 \end{cases} \tag{16}$$

This implies that the discontinuity occurs at the location of the crack. The branch function B_l is defined by

$$B_l(r,\theta)=\left\{\sqrt{r}\sin\frac{\theta}{2},\ \sqrt{r}\cos\frac{\theta}{2},\ \sqrt{r}\sin\frac{\theta}{2}\sin\theta,\ \sqrt{r}\cos\frac{\theta}{2}\sin\theta\right\} \tag{17}$$

where (r,θ) is a polar co-ordinate system with its origin at the crack tip and $\theta=0$ tangent to the crack at its tip. The above functions span the asymptotic crack tip solution of elasto-statics, and $\sqrt{r}\sin\frac{\theta}{2}$ takes into account the discontinuity across the crack face.

The introduction of the discrete approximation (15) into the principle of virtual work given by Equation (10) leads to a system of linear equations. The stress intensity factors are computed using the domain form of the J-integral as described in Reference [14]. The direction in which the crack will propagate from its current tip, θ_c, is obtained using the maximum hoop stress criteria [1]. The angle θ_c depends on the stress intensity factors, K_1 and K_2, and is given by

$$\theta_c=2\arctan\frac{1}{4}\left(\frac{K_1}{K_2}\pm\sqrt{\left(\frac{K_1}{K_2}\right)^2+8}\right),\quad -\pi<\theta_c<\pi \tag{18}$$

5. LEVEL SET ALGORITHM FOR MODELLING CRACK GROWTH

We model one-dimensional crack growth in a level set framework by representing the crack as the zero level set of a function $\psi(\mathbf{x},t)$. An endpoint of the crack is represented as the intersection of the zero level set of ψ with an orthogonal zero level set of the function $\phi_i(\mathbf{x},t)$, where i is the number of tips on a given crack. For cracks that are entirely in the interior of the bulk of a material, two functions are used, ϕ_1 and ϕ_2, one for each crack tip. For edge cracks only one function, ϕ_1, is necessary. The values of the level set functions are stored only at the nodes. The functions are interpolated over the mesh by the same shape functions as the displacement. Thus,

$$\phi_i(\mathbf{x},t)=\sum_{j\in J}\phi_{ij}(t)N_j(\mathbf{x});\qquad (\mathbf{x},t)=\sum_{j\in J}\psi_j(t)N_j(\mathbf{x}) \tag{19}$$

Since the shape functions are C^0, the crack representation is also C^0.

The level set function representing the initial crack is constructed by computing the signed-distance function for the crack. A difficulty in doing this arises from the fact that, although the crack tip lies within the domain, the level set function representing the crack must initially be constructed on the entire domain. To circumvent this problem, the initial crack is extended tangentially from its tip and the signed-distance function (14) is constructed from this extended crack.

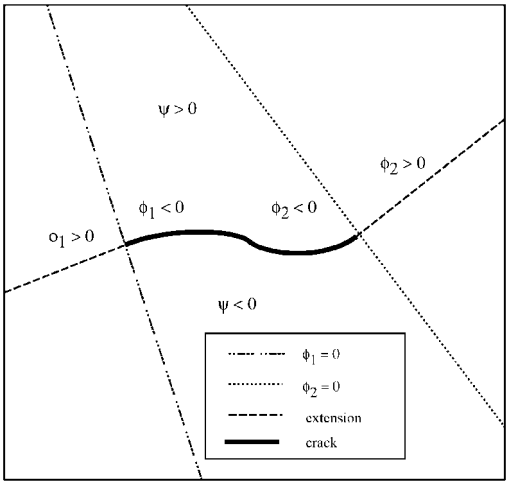

Figure 3. Construction of initial level set functions.

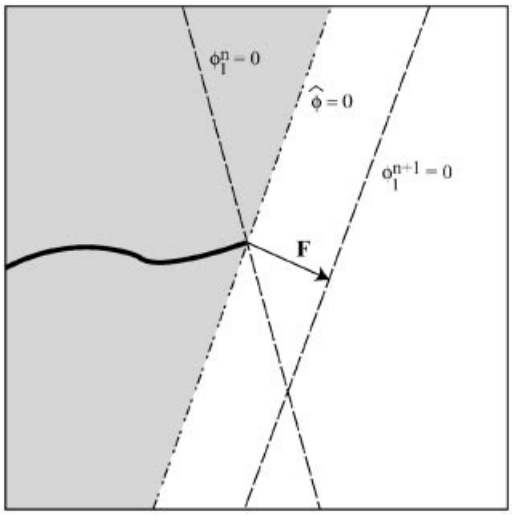

Figure 4. Level set function update. Gray region is $\Omega^{\text{no update}}$. Non-gray is Ω^{update}.

The level set functions that represent the crack tip are initially defined by

$$\phi_i(\mathbf{x},0) = (\mathbf{x} - \mathbf{x}_i)\cdot\hat{\mathbf{t}} \tag{20}$$

where $\hat{\mathbf{t}}$ is a unit vector tangent to the crack at its tip and $\mathbf{x}_i$ is the location of the ith crack tip. Given the construction described by (20), the planar function ϕ_i has a zero level set which is orthogonal to ψ at the crack tip. The initial level set functions, ψ and ϕ_i, and the representation of the crack are shown in Figure 3.

An important consideration is that, although the actual crack is embedded inside a domain, the zero level set of ψ cuts through the entire domain. In the level set framework, the crack is considered to be the zero level set of ψ, where both $\phi_1 \leqslant 0$ and $\phi_2 \leqslant 0$ in the case of an interior crack. In the case of an edge crack, $\phi_1 \leqslant 0$. This is consistent with the initial conditions and will continue to be so as the level set functions are updated.

For the case of more than one crack tip, it is convenient to define a single function $\phi(\mathbf{x},t)$ for the crack tip level set representation by

$$\phi(\mathbf{x},t) = \max_i(\phi_i) \tag{21}$$

The function ϕ allows us to define the location of the crack using only one function whether a crack has one or two tips. In other words, a crack is defined as the set

$$\{\mathbf{x} : \psi(\mathbf{x},t) = 0 \text{ and } \phi(\mathbf{x},t) \leqslant 0\} \tag{22}$$

As mentioned in Section 3, it is not necessary to update the level sets on the entire two-dimensional domain since we are only interested in the evolution of a one-dimensional curve. Thus, we can confine the level set representation to a narrow band of elements around the

crack. In addition, we assume that once a part of a crack has formed, that part will no longer change shape or move. Therefore, the ψ, ϕ_i, and ϕ functions need only be updated on a small region of elements surrounding each crack tip. This narrow band is built by surrounding the crack tip by a predetermined layer of elements. The number of surrounding elements is chosen so that it is larger than the incremental growth length of the crack.

Crack growth is modelled by appropriately updating the ϕ_i and ψ functions, then reconstructing the updated ϕ function. A crack is extended at each tip in the same manner, regardless of the number of cracks and the number of tips on a given crack. The evolution of ϕ_i and ψ is determined by the crack growth direction, θ_c. In each step, the displacement of the crack tip is given by the prescribed vector $\mathbf{F}=(F_x,F_y)$. The magnitude of crack extension $\|\mathbf{F}\|$ depends on the crack growth law. The current location of the crack tip, $\mathbf{x}_i=(x_i,y_i)$, is also used in the equations of evolution.

Let the current values of ϕ_i and ψ at step n be ϕ_i^n and ψ^n. The algorithm for the evolution of the level set functions ϕ_i and ψ is as follows:

(1) ϕ_i^n is updated using Equation (12). In Equation (12), F is always the speed normal to the interface. However, $\mathbf{F}$ is not necessarily orthogonal to the zero level set of ϕ_i^n. For this reason, we must first rotate ϕ_i^n so that $\mathbf{F}$ is orthogonal. ϕ_i^n after rotation is referred to as $\hat{\phi}_i$ and given by

$$\hat{\phi}_i=(x-x_i)\frac{F_x}{\|\mathbf{F}\|}+(y-y_i)\frac{F_y}{\|\mathbf{F}\|} \tag{23}$$

(2) The crack is extended by computing new values of ψ^{n+1} only where $\hat{\phi}_i>0$, which is referred to as Ω^{update}. Let the region where $\hat{\phi}_i\leqslant 0.0$ be $\Omega^{\text{no update}}$.

$$^{n+1}=\psi^n \quad \text{in } \Omega^{\text{no update}} \tag{24}$$

$$\begin{aligned} ^{n+1} &= \pm\left|(\mathbf{x}-\mathbf{x}_i)\times\frac{\mathbf{F}}{\|\mathbf{F}\|}\right| \\ &= \pm\left|(x-x_i)\frac{F_y}{\|\mathbf{F}\|}-(y-y_i)\frac{F_x}{\|\mathbf{F}\|}\right| \quad \text{in } \Omega^{\text{update}} \end{aligned} \tag{25}$$

The sign of ψ^{n+1} in Ω^{update} is chosen so that it is consistent with the current sign on a given side of the crack in $\Omega^{\text{no update}}$.

(3) ϕ_i^{n+1} is computed using (12) so that it represents the updated location of the crack tip.

$$\phi_i^{n+1}=\hat{\phi}-\Delta t\|\mathbf{F}\| \tag{26}$$

where, by construction, $\|\nabla\phi\|\equiv 1$ at all times. The rotated level set function $\hat{\phi}_i$ is calculated exactly in Equation (23). Since ϕ_i^{n+1} is calculated from $\hat{\phi}_i$, it is important to note that ϕ_i^{n+1} is also recalculated in each step rather than updated from the previous values of ϕ_i. The recalculation of ϕ_i^n to ϕ_i^{n+1} is illustrated in Figure 4.

(4) Once all ϕ_i^{n+1}'s corresponding to a crack are updated, ϕ^{n+1} is updated using (21).

The location of the new crack tip i can now be determined by finding the intersection of the zero level sets of ϕ_i^{n+1} and the newly extended ψ^{n+1}. The updated tip is used to determine a new region of elements over which the level set computation will take place.

6. COUPLING THE LEVEL SET METHOD AND THE EXTENDED FINITE ELEMENT METHOD

The LSM and X-FEM couple naturally to model crack growth. The algorithm for the growth of cracks given in Section 5 is simple to implement. The values of ψ, ϕ_i, and ϕ are stored at nodes. Any information needed for crack growth, such as the location of the crack tip, can be obtained from these nodal values, making it unnecessary to store any other information pertaining to the crack. The X-FEM algorithm is an efficient finite element scheme that solves the elliptical problem which determines the evolution of a crack on a mesh. The mesh is unchanged throughout the computation of the evolution of the crack. For these reasons, the LSM and X-FEM work quite well together.

Moreover, the level set representation of the crack facilitates the computation of the enrichment. The enrichment function (16) is defined so that the discontinuity is coincident with the crack. Because the crack is represented as the zero level set of ψ, all values above or below the crack are either positive or negative. From (16) we can see that

$$H(y) = H^*(\psi(\mathbf{x},t)) = \begin{cases} 1 & \text{for } \psi(\mathbf{x},t) > 0 \\ -1 & \text{for } \psi(\mathbf{x},t) < 0 \end{cases} \tag{27}$$

Therefore, to determine the location of a point relative to the crack, one merely has to determine the sign of ψ at that point.

The enrichment functions (17) are defined in co-ordinates local to the crack tip. These co-ordinates can be determined by the level set function representing the tip. The function associated with the tips, ϕ, is always planar with $\|\nabla\phi\| = 1$, and its zero level set is orthogonal to the zero level set of ψ at the crack tips. The orthogonality of these two level sets makes a natural co-ordinate system. The direction of the local x-axis is determined by $\nabla\phi$. The direction of the local y-axis is then simply $\hat{\mathbf{e}}_z \times \nabla\phi$, where $\hat{\mathbf{e}}_z = (0,0,1)$. In this local co-ordinate system, the arguments of the branch function (17) can be expressed by the level set functions. That is, at point $\mathbf{x}$, the radius from the crack tip and the angle of deviation from the tangent to the crack tip is given by

$$r = \sqrt{\ ^2(\mathbf{x},t) + \phi^2(\mathbf{x},t)} \quad \text{and} \quad \theta = \tan^{-1}\frac{(\mathbf{x},t)}{\phi(\mathbf{x},t)} \tag{28}$$

The nodes chosen for enrichment can be determined from the nodal values of ψ and ϕ. In a given element, let $\psi_{\min}$ and $\psi_{\max}$, respectively, be the minimum and maximum nodal values of ψ on the nodes of that element. If $\phi < 0$ and $\psi_{\min}\psi_{\max} \leqslant 0$, then the crack cuts through the element and the nodes of the element are to be enriched with (16). Similarly, let $\phi_{\min}$ and $\phi_{\max}$, respectively be the minimum and maximum nodal values of ϕ on the nodes of an element. If in that element $\phi_{\min}\,\phi_{\max} \leqslant 0$ and $\psi_{\min}\,\psi_{\max} \leqslant 0$, then the tip lies within that element, and its nodes are to be enriched with (17).

The coupling of the LSM with X-FEM is illustrated in Figure 5. For a given crack, each iteration begins by examining the level set functions at each node of each element in the narrow band and choosing the nodes which require enrichment from the nodal values of these functions. These nodes are then enriched by the appropriate function and the stress field is

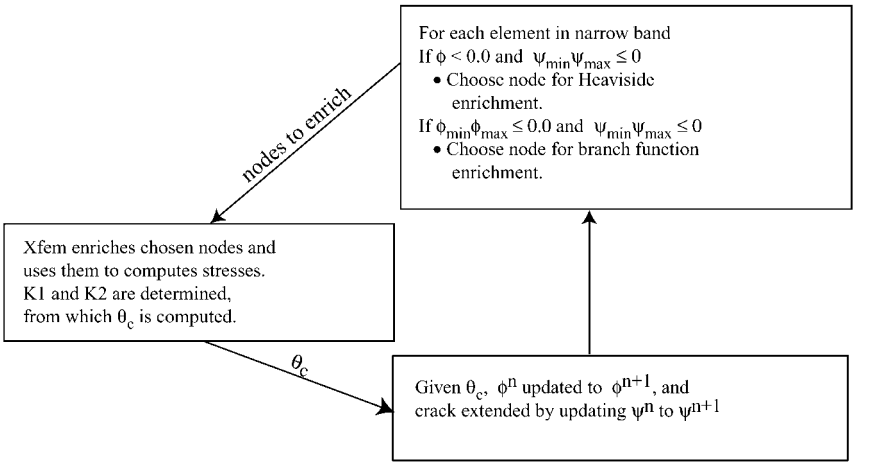

Figure 5. Coupling of the extended finite element method and the level set method.

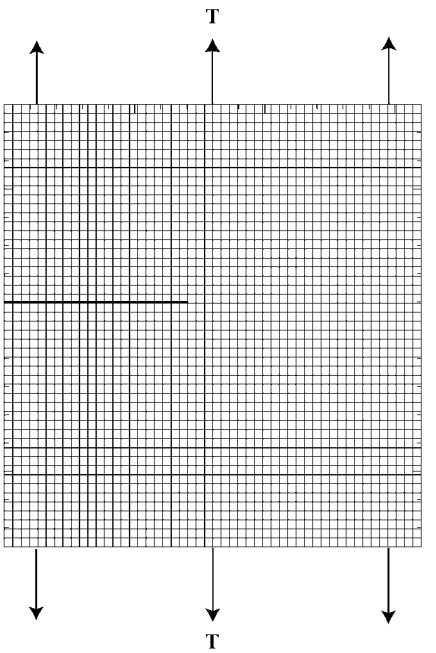

Figure 6. Initial configuration of edge crack problem.

determined by X-FEM. Once the stress field is determined, the stress intensity factors are computed, and from these factors the direction of crack growth θ_c is computed. The angle θ_c is then used in updating the level set functions. Once the level set functions are updated, the process is repeated.

7. NUMERICAL EXAMPLES

In this section we present three numerical examples. The first two examples present the growth of an initially straight crack in a simple square mesh subject to tensile loading. The third example illustrates the growth of a crack in a fillet of a structural member.

7.1. Crack growth in square mesh subject to tensile loading

The first two examples are chosen to illustrate the accuracy and robustness of the level set representation of crack growth. The first example is an edge crack, which has one moving endpoint. The other is a centre crack in which both endpoints are free to evolve. Both examples are run on a square mesh, where $x \in (0, 16)$ and $y \in (-8, 8)$. A cyclic traction normal to the edge is applied at $y = -8.0$, $0.0 \leqslant x \leqslant 16.0$ and at $y = 8.0$, $0.0 \leqslant x \leqslant 16.0$. The remaining boundaries are traction free. In addition, the lower left-hand corner of the mesh, $(0.0, -8.0)$, is fixed. The examples are run for a total of five steps, and in each step the crack grows a distance of 0.5 at each endpoint. The number of cycles per iteration is then obtained from the stress intensity factor by the Paris Law. The results obtained from the LSM are compared to those of the X-FEM algorithm described in Reference [1], where a crack is explicitly represented as a set of straight segments.

7.1.1. Edge crack. The first example is an edge crack under tensile loading $\mathbf{T}$ with unit amplitide. The co-ordinates of the endpoints of the initial crack are $(0.0, 1.0)$ and $(7.0, 1.0)$. This is illustrated in Figure 6. Stress intensity factors K_1 and K_2, as well as the location of crack tips, were compared for meshes of different refinement. The stress intensity factors are those computed *before* the crack grows for the given step. The comparison of the stress intensity factors is given in Table I, and the comparison of the crack tips is in Table II.

The level set representation of a crack is shown in Figure 7. The crack in this figure was modelled on a 50×50 mesh. The narrow band on which computation took place extends five elements around either side of the crack. The crack is represented by $\psi = 0$, which is drawn as the thicker line. In the level set representation, the crack tip is the intersection of the orthogonal zero level sets ψ and ϕ_i. For comparison, the solution determined by the explicit representation of the crack by a series of rectilinear line segments as described in Reference [1] is shown. The level set crack is semi-quadratic in each element because the shape function representation (22) is bilinear in each element.

Figure 8 shows the level sets of the functions representing the crack and the crack tip after the fifth iteration. It is clear from this figure that the zero level set of the ψ function represents the crack. The displayed level sets were chosen so that an approximate computational domain can be seen. Hence, the level set functions do not exist outside of the regions illustrated in Figure 8, and at each iteration, computation is done only in the region represented by the level sets of the function ϕ_1.

7.1.2. Centre crack. This example is again a crack in a plate under tensile loading $\mathbf{T}$ with unit amplitide, as shown in Figure 9. The initial crack is straight and has endpoints with co-ordinates (5.0, –1.0), referred to as tip 1, and $(11.0, 1.0)$, which is tip 2. The comparison of the stress intensity factors is shown in Table III, and the comparison of the crack tips is shown in Table IV.

Table I. Stress intensity factors for the edge crack.

Step	Explicit crack	Level set crack
30×30 *Mesh*		
1	K_1: 11.9437	K_1: 11.9437
	K_2: − 5.27453e − 1	K_2: − 5.27453e − 1
2	K_1: 13.4528	K_1: 13.4508
	K_2: − 7.19400e − 2	K_2: − 6.28707e − 3
3	K_1: 15.0378	K_1: 15.1149
	K_2: − 6.59637e − 2	K_2: − 4.16088e − 2
4	K_1: 16.9723	K_1: 17.0019
	K_2: 3.47538e − 2	K_2: − 3.06219e − 2
5	K_1: 19.3645	K_1: 19.3840
	K_2: 3.09982e − 2	K_2: − 1.10077e − 2
100 × 100 *Mesh*		
1	K_1: 11.9945	K_1: 11.9945
	K_2: − 5.69560e − 1	K_2: − 5.69560e − 1
2	K_1: 13.5723	K_1: 13.5723
	K_2: − 3.46207e − 2	K_2: − 3.45084e − 2
3	K_1: 15.3164	K_1: 15.3164
	K_2: − 5.70880e − 2	K_2: − 5.71534e − 2
4	K_1: 17.2541	K_1: 17.2459
	K_2: 9.49401e − 4	K_2: 3.45291e − 3
5	K_1: 19.4749	K_1: 19.4748
	K_2: 1.34399e − 2	K_2: 1.09760e − 2

Table II. Evolution of crack tips for the edge crack.

Step	Explicit crack	Level set crack
30×30 *Mesh*		
0	(7.00 000, 1.00 000)	(7.00 000, 1.00 000)
1	(7.49 807, 1.04 391)	(7.49 807, 1.04 391)
2	(7.99 564, 1.09 314)	(7.99 610, 1.08 828)
3	(8.49 276, 1.14 673)	(8.49 387, 1.13 539)
4	(8.99 009, 1.19 828)	(8.99 147, 1.18 429)
5	(9.48 759, 1.24 825)	(9.48 902, 1.23 376)
100×100 *Mesh*		
0	(7.00 000, 1.00 000)	(7.00 000, 1.00 000)
1	(7.49 777, 1.04 717)	(7.49 777, 1.04 717)
2	(7.99 529, 1.09 687)	(7.99 529, 1.09 687)
3	(8.49 243, 1.15 029)	(8.49 243, 1.15 028)
4	(8.98 958, 1.20 365)	(8.98 959, 1.20 349)
5	(9.48 679, 1.25 632)	(9.48 681, 1.25 614)

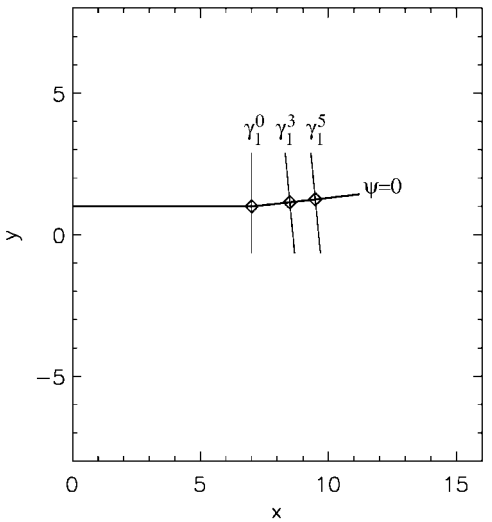

Figure 7. Edge crack at time $= 0, 3, 5$; γ_i^n corresponds to the zero level set of $\phi_i(\mathbf{x}, t_n)$. The explicit piecewise-linear representation is shown as the diamond.

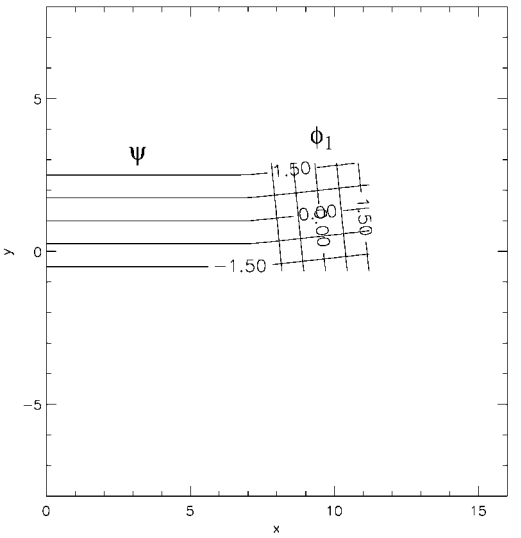

Figure 8. Level set functions representing the edge crack at time $= 5$.

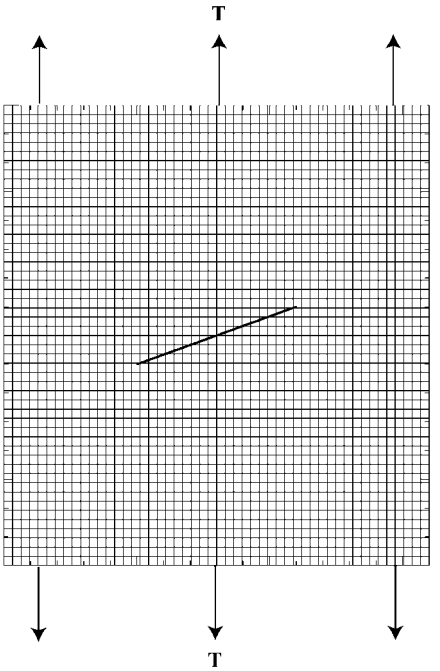

Figure 9. Initial configuration of centre-crack problem.

Table III. Stress intensity factors for centre crack.

Step	Explicit crack	Level set crack
30×30 *Mesh*—Tip 1 and Tip 2		
1	K_1: 3.42434	K_1: 3.42434
	K_2: 1.10835	K_2: 1.10835
2	K_1: 3.95943	K_1: 4.13820
	K_2: − 9.42231e − 1	K_2: − 6.40598e − 1
3	K_1: 4.55955	K_1: 4.76276
	K_2: 9.88267e − 1	K_2: 4.55367e − 1
4	K_1: 5.30417	K_1: 5.39151
	K_2: − 8.41266e − 1	K_2: − 3.45293e − 1
5	K_1: 5.97014	K_1: 6.11876
	K_2: 6.70257e − 1	K_2: 1.69089e − 1
100×100 *Mesh*—Tip 1		
1	K_1: 3.42837	K_1: 3.42837
	K_2: 1.08407	K_2: 1.08407
2	K_1: 4.21270	K_1: 4.21257
	K_2: −4.16980e − 1	K_2: −4.15402e − 1
3	K_1: 4.84677	K_1: 4.84653
	K_2: 6.94297e − 2	K_2: 6.74268e − 2
4	K_1: 5.43278	K_1: 5.43243
	K_2: −7.04901e − 2	K_2: −6.98822e − 2
5	K_1: 6.13437	K_1: 6.13395
	K_2: −7.43117e − 3	K_2: −7.74329e − 3
100×100 *Mesh*—Tip 2		
1	K_1: 3.42832	K_1: 3.42832
	K_2: 1.08403	K_2: 1.08403
2	K_1: 4.21262	K_1: 4.21249
	K_2: −4.16918e − 1	K_2: −4.15340e − 1
3	K_1: 4.84663	K_1: 4.84639
	K_2: 6.93549e − 2	K_2: 6.73526e − 2
4	K_1: 5.43255	K_1: 5.43219
	K_2: −7.04848e − 2	K_2: −6.98774e − 2
5	K_1: 6.13399	K_1: 6.13357
	K_2: −7.56382e − 3	K_2: −7.87572e − 3

The level set representation of the centre crack is shown is Figure 10. As in the first example, the crack is represented as the zero level set of a single function ψ. However, in this case, each endpoint is represented by a separate level set function, ϕ_1 and ϕ_2. The level sets of the three functions and an approximate computational domain are illustrated in Figure 11. Again, the cracks in both figures were modelled on a 50×50 mesh with a narrow band size of five elements on either side of the crack.

As can be seen in the tables, the results obtained from the LSM agree closely with those based on the explicit X-FEM representation. As the mesh is refined, the results converge towards one another. The slight discrepancy between the results of the two methods is caused mainly by a difference in the construction of the subelements [1], which are used for quadrature around the crack. In the case of the explicit representation, the crack is represented in a way

Table IV. Evolution of crack tips for the centre crack.

Step	Explicit crack	Level set crack
30×30 *Mesh*		
0	Tip 1: (5.00000, −1.00000)	Tip 1: (5.00000, −1.00000)
	Tip 2: (11.0000, 1.00000)	Tip 2: (11.0000, 1.00000)
1	Tip 1: (4.51147, −0.893528)	Tip 1: (4.51147, −0.893527)
	Tip 2: (11.4885, 0.893528)	Tip 2: (11.4885, 0.893528)
2	Tip 1: (4.02251, −0.998004)	Tip 1: (4.01304, −0.933143)
	Tip 2: (11.9775, 0.998004)	Tip 2: (11.9870, 0.933143)
3	Tip 1: (3.53088, −0.906860)	Tip 1: (3.51595, −0.879257)
	Tip 2: (12.4691, 0.90680)	Tip 2: (12.4840, 0.879257)
4	Tip 1: (3.03431, −0.965267)	Tip 1: (3.01604, −0.888707)
	Tip 2: (12.9657, 0.965269)	Tip 2: (12.9840, 0.888707)
5	Tip 1: (2.53686, −0.914761)	Tip 1: (2.51637, −0.870576)
	Tip 2: (13.4631, 0.914761)	Tip 2: (13.4836, 0.870576)
100×100 *Mesh*		
0	Tip 1: (5.00000, −1.00000)	Tip 1: (5.00000, −1.00000)
	Tip 2: (11.0000, 1.00000)	Tip 2: (11.0000, 1.00000)
1	Tip 1: (4.51055, −0.897817)	Tip 1: (4.51055, −0.897817)
	Tip 2: (11.4894, 0.897821)	Tip 2: (11.4894, 0.897821)
2	Tip 1: (4.01059, −0.891720)	Tip 1: (4.01059, −0.891372)
	Tip 2: (11.9894, 0.891716)	Tip 2: (11.9894, 0.891368)
3	Tip 1: (3.51101, −0.871310)	Tip 1: (3.51101, −0.871026)
	Tip 2: (12.4890, 0.871314)	Tip 2: (12.4890, 0.871030)
4	Tip 1: (3.01106, −0.863865)	Tip 1: (3.01106, −0.863534)
	Tip 2: (12.9889, 0.863875)	Tip 2: (12.9889, 0.863545)
5	Tip 1: (2.51110, −0.857631)	Tip 1: (2.51110, −0.857305)
	Tip 2: (13.4889, 0.85767)	Tip 2: (13.4889, 0.857343)

such that the crack can kink inside an element. However, the level set functions are defined at the nodes of elements, allowing only for a smooth interpolation, as given in Equation (19), of the level sets within each element. The subelements in the level set geometry are therefore constructed on either side of a smooth crack, whereas subelements in the explicit representation are constructed so that they match the geometry of the kinks. Additionally, in the explicit representation of the crack, subelements can be built within existing subelements. In the level set representation, at each iteration all of the existing subelements are deleted and a completely new set is created. These differences in subelements cause unequal quadrature near the crack tip, which in turn causes a slight difference between the evolutions of the explicit and level set cases. As the mesh is refined, the need for reslicing elements as well as the fraction of elements in which kinks can occur is reduced, making the subelements in the two methods more comparable.

7.2. Crack growth from a fillet

This example shows the growth of a crack from a fillet in a structural member. The configuration of the problem is taken from experimental work found in Reference [15] and is shown in

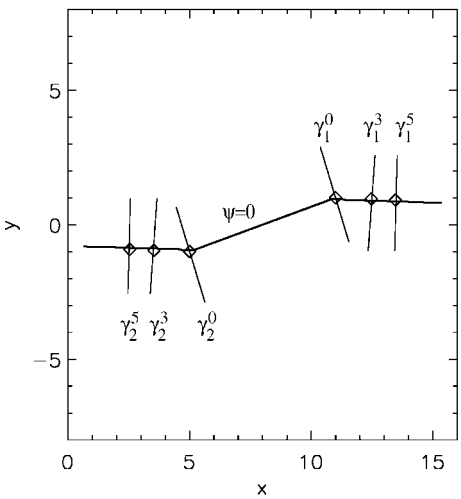

Figure 10. Centre crack at time $= 0, 3, 5$; γ_i^n corresponds to the zero level set of $\phi_i(\mathbf{x}, t_n)$. The explicit piecewise-linear representation is shown as the diamond.

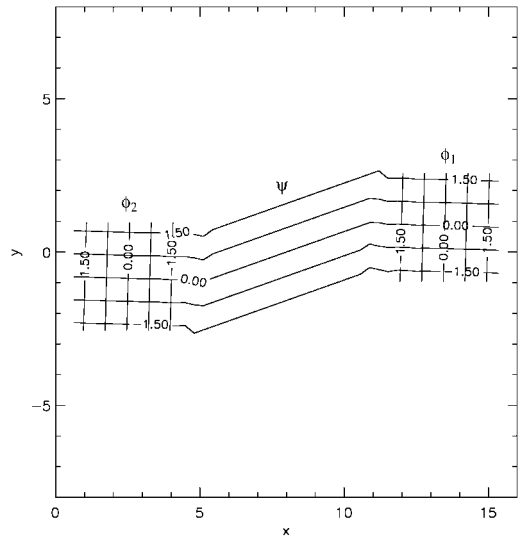

Figure 11. Level set functions representing the centre crack at time $= 5$.

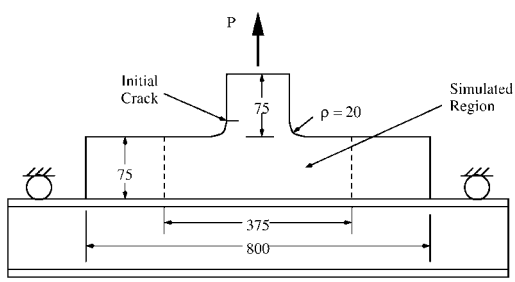

Figure 12. Experimental configuration of crack growth from a fillet taken from Reference [15].

Figure 12. The computational domain is outlined by the dashed line. In this example, we investigate the effects of the thickness of the lower I-beam. Only the limiting cases of a very thick, rigid I-beam and a very thin, flexible I-beam are discussed. The effects of the thickness are incorporated into the problem through the boundary conditions. For a rigid beam, the displacement in the vertical direction is fixed on the entire bottom. To model a flexible beam we fix the vertical displacement of only the endpoints of the bottom of the domain. The structure is loaded at the top boundary with a load of $P = 20$ kN.

The initial crack is 5 mm in length. Crack growth was simulated for a total of 12 steps, with each step size of length 5 mm. The narrow band on which the level set functions are computed extends four elements on either side of the crack. Figure 13 is a close-up of the mesh in the

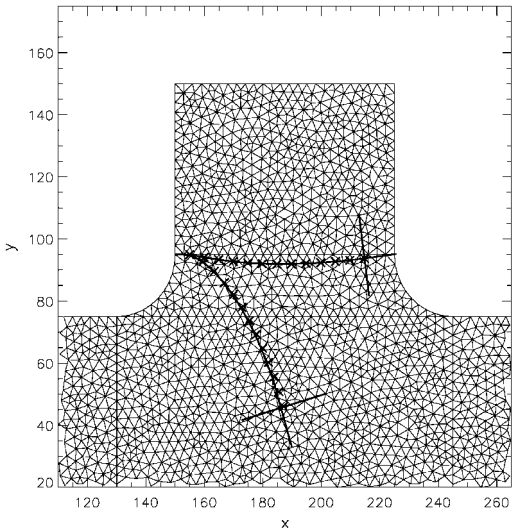

Figure 13. Crack paths for a rigid (upper crack) and flexible (lower crack) constraint. The path of the level set solution is shown as the solid line with the crack tip at the twelfth step shown as the intersection of the two zero level sets. The path of the explicit crack is shown by an X at the crack tip for each step.

vicinity of the fillet. Crack paths for a rigid constraint (upper path) and flexible constraint (lower path) are shown for both the level set representation and the explicit piecewise-linear representation. The crack model given by the level sets in this case is piecewise linear since triangular elements with linear shape functions are used for Equation (22). However, the length of the segments is determined by the elements encountered by the crack path. The crack tip at the twelfth step is the intersection of $\psi = 0$ and the orthogonal solid line $\phi = 0$. The explicit representation is shown as an X at the crack tip location at each iteration.

8. CONCLUSIONS

The LSM and X-FEM couple naturally to solve the elasto-static fatigue crack problem. The level set formulation is used to model the crack and update the crack tip at each iteration. The geometry of the crack is easily represented by two zero level sets that are orthogonal to one another at the crack tip. The level set functions, therefore, naturally provide two local co-ordinate systems that are needed for enrichment by the X-FEM algorithm. The process of determining the nodes to be enriched is facilitated through the level set representation. We use X-FEM to solve the elasto-static problem and determine the direction of crack growth. The examples presented show that the results obtained by the level set formulation are comparable to those obtained with an explicit model of the crack. The advantages of the LSM and the X-FEM, although not overwhelming in two dimensions, are simple and useful. In three dimensions, the advantages of the combination of the two methods promise to be very beneficial.

ACKNOWLEDGEMENTS

The support of the Office of Naval Research of T. Belytschko and N. Moës is gratefully acknowledged.

REFERENCES

1. Moës N, Dolbow J, Belytschko T. A finite element method for crack growth without remeshing. *International Journal for Numerical Methods in Engineering* 1999; **46**:131–150.
2. Belytschko T, Black T. Elastic crack growth in finite elements with minimal remeshing. *International Journal for Numerical Methods in Engineering* 1999; **45**:601–620.
3. Belytschko T, Moës N, Usui S, Parimi C. Arbitrary discontinuities in finite elements. *International Journal for Numerical Methods in Engineering* 2001; **50**(4):993–1013.
4. Osher S, Sethian JA. Fronts propagating with curvature dependent speed: algorithms based on Hamilton–Jacobi formulations. *Journal of Computational Physics* 1988; **79**(1):12–49.
5. Smereka P. Spiral crystal growth. *Physica D* 2000; **138**:282–301.
6. Oliver J. Continuum modeling of strong discontinuities in solid mechanics using damage models. *Computational Mechanics* 1995; **17**:49–61.
7. Oliver J. Modelling strong discontinuities in solid mechanics via strain softening constitutive equations. Part 2: numerical simulations. *International Journal for Numerical Methods in Engineering* 1996; **39**:3601–3623.
8. Armero F, Garikipati K. Analysis of strong-discontinuities in inelastic solids with applications to the finite element simulation of strain localization problems. *Proceedings of Engineering Mechanics* 1996; **1**:136–139.
9. Duarte CA, Hamzeh N, Liszka TJ, Tworzydlo WW. A generalized finite element method for the simulation of three-dimensional dynamic crack propagation. *Computer Methods in Applied Mechanics and Engineering* 2001; **190**(15-17):2227–2262.
10. Belytschko T, Lu YY, Gu L. Element-free Galerkin methods. *International Journal for Numerical Methods in Engineering* 1994; **37**:229–256.
11. Sukumar N, Chopp DL, Moës N, Belytschko T. Modeling holes and inclusions by level sets in the extended finite element method. *Computer Methods in Applied Mechanics and Engineering* 2001; in press.
12. Sukumar N, Chopp DL, Moran B. Extended finite element method and fast marching method for three-dimensional fatigue crack propagation. *Journal of Computational Physics* 2001; submitted for publication.
13. Chopp DL. Computing minimal surfaces via level set curvature flow. *Journal of Computational Physics* 1993; **106**:77–91.
14. Moran B, Shih CF. Crack tip and associated domain integrals from momentum and energy balance. *Engineering Fracture Mechanics* 1987; **27**:615–641.
15. Sumi Y, Yang C, Wang Z. Morphological aspects of fatigue crack propagation. Part II—effects of stress biaxiality and welding residual stresses. *Technical Report*. Department of Naval Architecture and Ocean Engineering, Yokohama National University, Japan, 1995.